NJC

Accepted Manuscript

This is an *Accepted Manuscript*, which has been through the Royal Society of Chemistry peer review process and has been accepted for publication.

Accepted Manuscripts are published online shortly after acceptance, before technical editing, formatting and proof reading. Using this free service, authors can make their results available to the community, in citable form, before we publish the edited article. We will replace this *Accepted Manuscript* with the edited and formatted *Advance Article* as soon as it is available.

You can find more information about *Accepted Manuscripts* in the Information for Authors.

Please note that technical editing may introduce minor changes to the text and/or graphics, which may alter content. The journal's standard Terms & Conditions and the Ethical guidelines still apply. In no event shall the Royal Society of Chemistry be held responsible for any errors or omissions in this *Accepted Manuscript* or any consequences arising from the use of any information it contains.

ROYAL SOCIETY OF CHEMISTRY

www.rsc.org/njc

Journal Name

ARTICLE

Influence of the Protonic State of an Imidazole-Phenanthroline Ligand on the Luminescence Properties of Copper(I) Complexes: Experimental and Theoretical Research

Received 00th January 20xx,
Accepted 00th January 20xx

DOI: 10.1039/x0xx00000x

www.rsc.org/

Xinfang Liu, [a] Rongfang Li,[a] Lufang Ma,[a] Xun Feng*[a] and Yuqiang Ding*[b]

Abstract: Two ionic (**1a** and **1b**) and two neutral (**2a** and **2b**) Cu(I) complexes containing un-deprotonated or deprotonated nitrogen ligand {2-(4-methyl phenyl) imidazole[4,5-f]-1,10- phenanthroline, MHPIP} and different phosphine ligands (bis[2-(diphenylphosphino) phenyl]ether and PPh_3) have been synthesized and characterized by elemental analysis, ^{1}H NMR spectroscopy and X-ray crystallography (**1b**, **2a** and **2b**). The complexes adopt a distorted tetrahedral geometry constructed by MHPIP (or $MPIP^-$) and phosphine ligand. The emission spectra show that the ionic complexes exhibit almost ignorable luminescence. However, deprotonation of the nitrogen ligand makes the neutral complexes exhibit orange or yellow emission both in solution and solid-powder states. Considering the different luminous characters of the neutral complexes, density functional theory (DFT) calculations have been performed at the B3LYP/6-31G** level to provide information about the impact of phosphine ligands on frontier orbit.

Introduction

In recent decades, much efforts have been devoted to the design and synthesis of copper(I) complexes due to the low cost and stable supply of the raw materials and their potential applications as luminescent materials[1]. In addition, the emission energies of the copper(I) complexes can cover the entire visible region with the change of ligand[2], so ligand strategy plays an important role in designing luminescent species. 1,10-Phenanthroline (1,10-phen) ligand has been extensively utilized to prepare metal complexes with attractive luminescence features[3]. However, $[Cu(1,10\text{-phen})_2]^+$ is a weakly emissive compound because a distortion from tetrahedral toward square planar geometry may occur and accelerate non-radiative decay of the excited-state[4]. Replacing one 1,10-phen with hindered phosphine ligand is an effective method to reduce excited state relaxation[5]. Another fruitful strategy involves the chemical functionalization of 1,10-phen at various ring positions [6]. For example, copper(I) (2,9-dialkyl-1,10-phenanthroline) units have been widely used to construct of photo- and electroactive devices[7].

However, such ligand are almost 2,9-substituted 1,10-phen and the chemical functionalization at other ring positions is still under development. Furthermore, the ligands are mostly used to prepare ionic complexes, more general copper(I) neutral complexes are rarely reported. Given this, we turn to 2-(4-methylbenzene) imidazo [4,5-f]-1,10-phen (MHPIP), a 5,6-substituted-1,10-phen-imidazole ligand, which combines the versatile structural and chemical properties of imidazole and 1,10-phen. So far, such ligands are mainly used as neutral ligand[8]. Occasionally, they are deprotonated to produce neutral complexes [9]. However, the impacts of protonic state on the luminescence properties of complexes are rarely comparatively studied except the synthesis of Ruthenium(II) complexes by Aukauloo et al[8]. We are curious whether the deprotonation of the 1,10-phen-imidazole ligand will influence the luminescence properties of copper(I) complexes, and how the ancillary ligand influence the emission characters.

Herein, we prepared two ionic and two neutral copper(I) complexes with MHPIP (or deprotonated MPIP) and DPEphos (or PPh_3) as *N*- and *P*-containing ligand, respectively, namely, $[Cu(MHPIP)(DPEphos)](BF_4)$ (**1a**), $[Cu(MHPIP)(PPh_3)_2](BF_4)$ (**1b**), Cu(MPIP)(DPEphos) (**2a**) and $Cu(MPIP)(PPh_3)_2$ (**2b**). Besides the synthesis and structural characterization, the absorption and

[a] College of Chemistry and Chemical Engineering, Luoyang Normal University, Luoyang, Henan, P. R. China
E-mail: fengx@lynu.edu.cn
School of Chemical and Material Engineering, Jiangnan University, Wuxi, Jiangsu, 214122, P. R. China.

† Electronic Supplementary Information (ESI) available: [Calculated Mulliken and NBO charges, frontier orbital of **2a** and **2b**, ^{1}H NMR spectra for **1a**, **1b**, **2a** and **2b**. CCDC reference numbers 1057666-1057668.]. See DOI: 10.1039/x0xx00000x

emission spectra of the complexes have also been studied. Considering the different luminescent characters, density functional theory (DFT) calculations of the neutral complexes have been performed at the B3LYP/6-31G** level to provide information about frontier orbital.

Results and Discussion

Syntheses

The synthesis of the mononuclear copper(I) complexes is outlined in Scheme 1. Reaction of precursor $Cu(CH_3CN)_4 \cdot BF_4$ with HMPIP and phosphine ligand give ionic complexes $[Cu(MHPIP)(DPEphos)] \cdot BF_4$ (**1a**) and $[Cu(MHPIP)(PPh_3)_2] \cdot BF_4$ (**1b**). By treating **1a** and **1b** with strong base (KOH), neutral complexes Cu(MPIP)(DPEphos) (**2a**) and Cu(MPIP) $(PPh_3)_2$ (**2b**) can be prepared and crystallized from anhydrous ether. The neutral complexes can also be prepared by the one-step reaction of the precursor, ligands and KOH (see Scheme 1). However, the one-step method prepares the neutral complexes in a lower yield than the two-step method because the precursor prefers to react with KOH which have been proven by the observation of black Cu_2O powder. During the deprotonation of MHPIP, KOH has been proven to be a better candidate than NaOH because K^+ matches well with BF_4^- in radius.

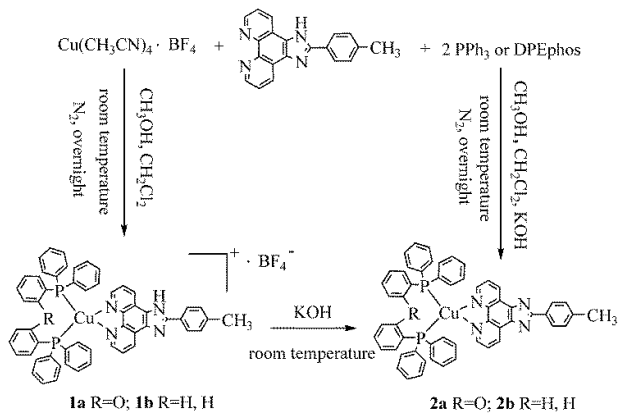

Scheme 1. The synthesis route of the ionic and neutral complexes

Crystal structures

To unambiguously elucidate the structures of the copper(I) complexes, X-ray diffraction analyses of complexes **1b**, **2a** and **2b** are carried out and the crystal structures are shown in Figures 1-3. The selected bond distances and bond angles are shown in Table 1. The Cu(I) center in all three complexes has a distorted tetrahedral geometry formed by two phosphorus atoms from two PPh_3 ligands (**1b** and **2b**) (or one DPEphos ligand, **2a**) and two nitrogen atoms from MHPIP (**1b**) (or MPIP anion, **2a** and **2b**). The Cu-N and Cu-P bond lengths are in the range of 2.060(2)-2.099(3) and 2.236(6)-2.297(7) Å, respectively, which are consistent with previously studied copper(I) complexes with the same or similar ligands[10].

For ionic complex **1b**, a $[Cu(PPh_3)_2(MHPIP)]^+$ ion cluster is formed when PPh_3 and MHPIP coordinate with the Cu(I) center. Two Cu(I) ion clusters are linked by two water and CH_3OH molecules through intermolecular hydrogen bonds (N4-H4…O1, 1.95(4) Å, 165(4)°; O1-H1D…O2, 1.96 Å, 163.1°; O2-H2…N3#1, 2.08 Å, 165.7°) to form a dimer (Figure 1b). In addition, strong intermolecular π-π interactions between the imidazole and benzene rings of the adjacent ion clusters (perpendicular distance: 3.378(9) Å; centroid distance: 3.916(1) Å) also play an important role in stabilizing the dimer unit [11]. The counter anion, BF_4^-, is linked to adjacent free water by weak intermolecular hydrogen bonds (O1-H1C…F4A, 2.01 Å, 173.3°; O1-H1C…F3B, 2.07 Å, 153.1°). And the BF_4^- anions stack with the ion clusters through ionic bonds.

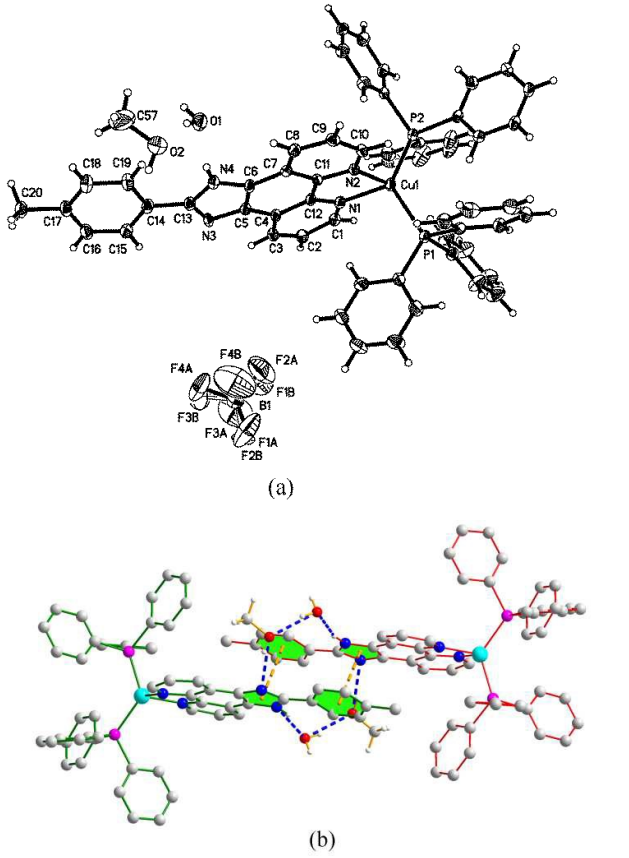

Figure 1. (a) ORTEP diagram of **1b** with thermal ellipsoids shown at the 30% probability level. (b) Hydrogen bonds and π-π interactions in **1b**.

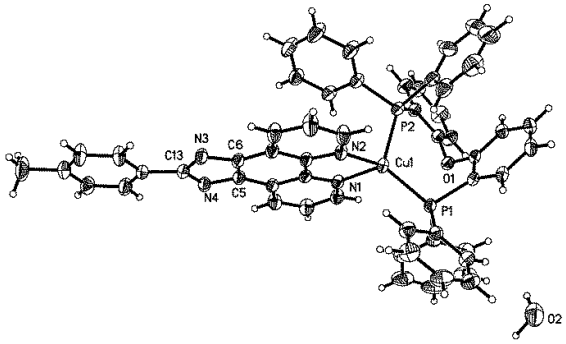

Figure 2. ORTEP diagram of complex **2a** with thermal ellipsoids shown at the 30% probability level.

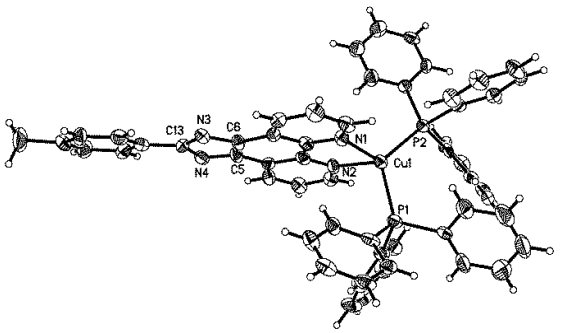

Figure 3. ORTEP diagram of complex **2b** with thermal ellipsoids shown at the 30% probability level.

Table 1. Selected bond distances and angles for **1b**, **2a** and **2b**

Bond length (Å)	1b	2a	2b
Cu(1)-N(1)	2.074(3)	2.060(2)	2.092(7)
Cu(1)-N(2)	2.099(3)	2.078(2)	2.097(8)
Cu(1)-P(1)	2.265(1)	2.236(6)	2.247(2)
Cu(1)-P(2)	2.286(1)	2.297(7)	2.284(2)
N(3)-C(13)	1.325(5)	1.346(3)	1.370(11)
N(3)-C(5)	1.384(5)	1.369(3)	1.382(10)
N(4)-C(13)	1.363(5)	1.359(3)	1.362(11)
N(4)-C(6)	1.365(5)	1.366(3)	1.366(10)
C(5)-C(6)	1.374(6)	1.392(4)	1.362(11)
Bond angles (°)	**1b**	**2a**	**2b**
N(1)-Cu(1)-N(2)	80.57(1)	80.85(8)	80.1(3)
N(1)-Cu(1)-P(1)	112.2(1)	118.7(6)	118.6(2)
N(1)-Cu(1)-P(2)	109.3(9)	106.6(6)	109.6(2)
P(2)-Cu(1)-P(1)	125.3(4)	115.8(2)	120.8(9)
P(2)-Cu(1)-N(2)	108.3(1)	101.7(6)	105.3(2)
P(1)-Cu(1)-N(2)	112.2(1)	127.2(6)	114.6(2)

For the neutral complexes (**2a** and **2b**) involving the same MPIP and different phosphine ligands, the bond lengths in Table 1 indicate that DPEphos meshes with MPIP better than PPh_3 because the average Cu-N distance of **2a** (2.069(2) Å) is distinctly shorter than that of **2b** (2.095(8) Å). In addition, the P-Cu-P angle in **2a** (115.8(2)º) presents a smaller distortion than that of **2b** (120.8(9)º) due to the presence of ether linkage of the DPEphos ligand. These results are all consistent with the findings of the previous studies [12].

The purities of complexes **1b**, **2a** and **2b** are determined by comparison of the simulated and experimental X-ray powder diffraction patterns, and the results are reported in Figure S1. The peak positions of the experimental patterns nearly matched with the simulated ones generated from the crystal structures, which indicates that the phases of three complexes are pure. The differences in intensity may be due to the preferred orientation of the microcrystalline powder samples

Absorption and emission spectra

The normalized absorption of the complexes in anhydrous ether are shown in Figure 4a. These complexes display two intense absorption bands from 230 to 320 nm, which have ascribed as ligand-to-ligand charge transfer (LLCT) transitions or intraligand charge transition (ILCT). The neutral complexes display an absorption peak (shown as a shoulder for **2b**) at about 335nm, while the peak of the ionic complexes are unobserved or obscure, indicating the influence of deprotonation on the absorption spectra. A weak low-energy band with maxima ranging from 380 to 480 nm is found. The absorption bands are obscure (especially for **2b**) owing to its small transition probability, *i.e.* the rather low absorptivity, which are analogous to those reported copper(I) complexes[13]. Different from the absorption bands before mentioned, the absorption peak between 380 and 480 nm changes with the *P*-, *N*-containing ligand. As suggested by TD-DFT studies (vide infra), the lowest-lying absorption bands of **2a** and **2b** are mainly assigned to LLCT and ILCT transition, respectively. The different transition may influence the emissive behaviour of the neutral complexes.

Emission spectra are measured at room temperature in different solvent. The results show that the complexes are not emissive in CH_2Cl_2 and CH_3OH. However, neutral complex **2b** exhibits an emission λ_{max} at 576 nm (yellow region) and **2a** shows a broad peak centered at 609 nm (orange region) (Figure 4a). The emission peak shifts toward higher energy with the ligand changing from PPh_3 to DPEphos. The trend of emission peaks is consistent with that of the low-energy absorptions shown in Figure 4a, illustrating that both spectra may originate from the same electronic excited state. According to the literatures, the tendency of the emission energies (**2b** > **2a**) is contrary to the electron-donating ability of the phosphine ligands (PPh_3 < DPEphos) and the same order as the P-Cu-P bond angles (120.8(9)° for **2b** and 115.8(2)° for **2a**, see Table 1)[1, 14]. The ionic complexes are slightly soluble in anhydrous ether, so it is difficult to determine their luminescence properties in solution.

Finally, the emission spectra in solid-powder states are explored to exclude the influences of solvent (Figure 4b). The results show that the neutral complexes exhibit luminescence at 612 nm for **2a** and at 580 nm for **2b**, which are actually close to their solution emissions. The emission peak of **2a** shows a remarkable red-shift (~32 nm) relative to that of **2b**. The red-shift may be caused by the introduction of the electron-

donating ether oxygen in DPEphos, raising the LUMO level, less influencing the HOMO energy (see Figure 5), thus decreasing the HOMO–LUMO gap[15]. The ionic complexes exhibit green luminescence (570 and 529nm for **1a** and **1b**, respectively), while the emission intensity is very weak.

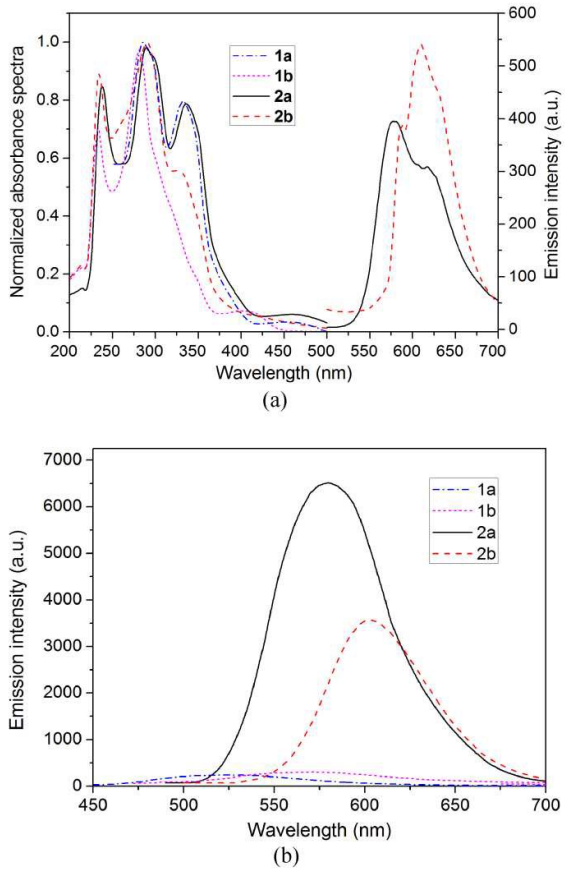

Figure 4. (a) Absorbance and emission spectra of the complexes in anhydrous ether. (b) Emission spectra of the complexes in powder states.

DFT calculations

To gain insight into the relationship between the electronic structure and luminescence properties of the neutral complexes, considering their excellent luminescence properties and their different emissive characters, density functional theory (DFT) calculations with the B3LYP/6-31G** method were performed.

To analyse the electronic structure more detailed, the Mulliken and the NBO charges have been determined [15] (Table S1 and Figure S2). These charges do not represent absolute charges but the trends among the complexes can impress the electronic effects. When compared with **2b**, the charges of the Phen-N atoms (N1 and N2) in **2a** are in average 0.007 (Mulliken charge) or 0.018 (NBO charge) more negative. In addition, the P atoms in **2a** are more positive (0.007 for Mulliken charge shows and for 0.023 NBO charge on average) than those of **2b**. The results preliminarily suggest that LLCT transition (MPIP→DPEphos) more likely occurs in **2a** which will be further illustrate by the following analysis of frontier orbital.

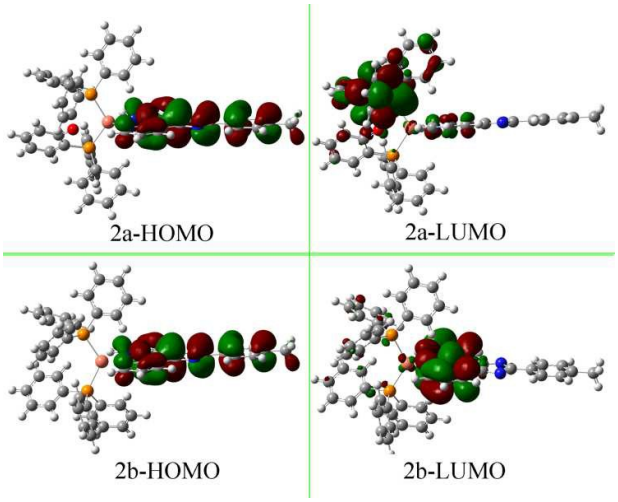

Figure 5. HOMO and LUMO diagrams of complexes **2a** and **2b**.

Table 2. Calculated absorption spectra of complexes **2a** and **2b**

	λ(nm)/E(eV)	f	main configurations	assignment
2a	498/2.84	0.0346	HOMO-1→LUMO (75.5%)	LLCT/ILCT/LMCT
	357/2.97	0.2305	HOMO-3→LUMO (8.8%) HOMO1→LUMO+6 (24.9%) HOMO→LUMO+8 (15.9%)	LLCT/ILCT/LMCT LLCT LLCT
	302/3.66	0.4888	HOMO-2→LUMO +5 (81.6%)	LLCT/ILCT
2b	495/3.12	0.0278	HOMO-1→LUMO (81.7%)	ILCT/LLCT/LMCT
	350/3.54	0.3270	HOMO-2→LUMO (38.6%) HOMO→LUMO+5 (15.5%)	ILCT/LLCT/LMCT LLCT/ILCT
	295/4.20	0.7752	HOMO-1→LUMO+1 (70.1%)	LLCT

The frontier orbital are shown in Figure 5, more figures on TD-DFT studies are provided in the Supporting Information (see Figures S3 and S4). The HOMO of **2a** and **2b** are mainly over the MPIP ligand (97.43% and 97.30%, respectively), and the HOMO-1, HOMO-2 and HOMO-3 are almost resident on MPIP. It is worth noting that the LUMO of **2a** and **2b** show large difference. For example, the LUMO of **2a** is mainly on DPEphos (71.62%) while partly on MPIP (22.40%) and Cu (5.98%); the LUMO of **2b** is mainly located on MPIP (83.18%), and less parts on PPh_3 (9.95%) and Cu (6.87%). Hence, the calculated lowest-energy absorption of **2a** at 458 nm from HOMO-

1→LUMO transition is of a significant LLCT transition (MPIP→DPEphos) character mixed with a certain degree of the intraligand (ILCT) transition and a small amount of LMCT transition (MPIP→Cu) [16]. Similarly, the lowest-energy absorption of **2b** is mainly assigned to ILCT transition and partly assigned to LLCT transition (MPIP→PPh_3) and LMCT transition (MPIP→Cu). In exactly the same way, the next two absorption bands of **2a** and **2b** have been assigned and listed in Table 2. Some subtle differences are observed about the molecular orbital configurations and assignment (Table 2) as well as the frontier molecular orbitals (Figures S3 and S4) of **2a** and **2b**, which can provide evidence for the different absorption and emission spectra before mentioned.

Conclusions

We have synthesized two ionic and two neutral mononuclear Cu(I) complexes bearing different protonic states of 1,10-phen-imidazole ligand. This paper describes the differences in the emission properties of the neutral and ionic complexes at ambient temperature. The emissive properties of the neutral complexes can change with the ancillary phosphine ligands as supported by detailed density functional theory calculations. The theory calculations can provide new insight into the synthesis of different colours of copper(I) phosphorescent materials via well modulating the structures of ligands.

Experimental Section

Materials

CuCl, DPEphos, PPh_3, 4-methyl benzaldehyde, 1,10-phen monohydrate, fluoroboric acid (HBF_4) and other chemicals were obtained from commercial sources and used without further purification. All solvents were dried by common methods and freshly distilled prior to use. 2-(4-methyl phenyl) imidazo[4,5-f]-1,10-phen were prepared according to the reported literature procedures [17]. $[Cu(CH_3CN)_4]BF_4$ was synthesized via the described procedure [18].

Experimental details

The synthetic procedures involving the reaction of Cu(I) species were carried out under a nitrogen atmosphere using a standard schlenk flask,considering the oxidative stability of the copper(I) complexes in the reactions.

Synthesis procedure

$[Cu(MHPIP)(DPEphos)]\cdot BF_4$ (**1a**): A CH_2Cl_2 solution of $Cu(CH_3CN)_4\cdot BF_4$ (0.032g, 0.1 mmol), MHPIP (0.031g, 0.1mmol) and DPEphos (0.054g, 0.1mmol) was stirred at room temperature overnight to give a yellow solution. The solution was filtered over celite and the solvent was removed by rotary evaporator. The residue was separated on TLC plates with a solvent of dichloromethane. The pure product was dissolved in anhydrous methanol and yellow block crystals (0.073g, 48%) were obtained by the solvent evaporation method. ^{1}H NMR (400 MHz, DMSO) (Figure S5): δ 8.69 (d, *J* = 7.9 Hz, 2H), 8.36 (d, *J* = 4.1 Hz, 2H), 7.94 (d, *J* = 6.8 Hz, 2H), 7.42 (dd, *J* = 8.0, 4.6 Hz, 2H), 7.31 – 7.14 (m, 4H), 7.10 – 7.04 (m, 6H), 6.99 (t, *J* = 7.4 Hz, 8H), 6.87 (t, *J* = 7.5 Hz, 2H), 6.76 (dd, *J* = 11.7, 5.6 Hz, 8H), 6.42 – 6.35 (m, 2H), 2.29 (s, 3H). Anal. Calcd for $C_{56}H_{42}BCuF_4N_4OP_2$: C, 67.31; H, 4.24; N, 5.61%. Found: C, 67.02; H, 4.18; N, 5.86%.

$[Cu(MHPIP)(PPh_3)_2]\cdot BF_4\cdot CH_3OH\cdot H_2O$ (**1b**): synthesized in the same way as **1a**, except that DPEphos (0.054g, 0.1mmol) was replaced by PPh_3 (0.053g, 0.2mmol). The yield of **1b** was 0.075g (56%). ^{1}H NMR (400 MHz, DMSO) (Figure S6): δ 14.02 (s, 1H), 9.08 (d, *J* = 5.2 Hz, 2H), 8.82 (s, 2H), 8.22 (d, *J* = 8.1 Hz, 2H), 7.90 (dd, *J* = 8.3, 5.7 Hz, 2H), 7.49 – 7.42 (m, 4H), 7.24 (ddd, *J* = 21.8, 14.9, 7.4 Hz, 16H), 7.10 (t, *J* = 7.5 Hz, 2H), 6.98 (dd, *J* = 12.1, 5.5 Hz, 8H), 6.67 (dt, *J* = 12.0, 4.6 Hz, 2H), 2.44 (s, 3H). Anal. Calcd for $C_{57}H_{50}BCuF_4N_4O_2P_2$: C, 66.12; H, 4.87; N, 5.41%. Found: C, 67.03; H, 4.95; N, 5.66%.

$[Cu(MPIP)(DPEphos)]\cdot H_2O$ (**2a**): CH_3OH (20mL) was added into a schlenk tube containing **1a**（0.102g, 0.1mmol）and KOH (0.006g, 0.1mmol) under nitrogen atmosphere. The mixture was stirred at room temperature overnight to give an orange solution. The solution was filtered and the solvent was removed by rotary evaporator. The residue was dissolved in anhydrous ether and orange block crystals were obtained by the solvent evaporation method (0.082g, 90%).^{1}H NMR (400 MHz, CD_2Cl_2) (Figure S7): δ 9.11 (d, J = 8.0 Hz, 2H), 8.41 (d, J = 4.3 Hz, 2H), 8.35 (d, J = 8.0 Hz, 2H), 7.45 (dd, J = 8.2, 4.7 Hz, 2H), 7.34 – 7.21 (m, 8H), 7.10 (t, J = 7.4 Hz, 10H), 7.00 (dt, J = 15.3, 6.3 Hz, 10H), 6.75 (dt, J = 6.1, 3.7 Hz, 2H), 2.40 (s, 3H). Anal. Calcd for $C_{56}H_{43}CuN_4P_2$: C, 74.94; H, 4.83; N, 6.24%; Found: C, 75.36; H, 4.96; N, 6.30%.

$Cu(MPIP)(PPh_3)_2$ (**2b**): synthesized in the same way as **2a**, except that DPEphos was replaced by PPh_3 (0.077g, 86%). ^{1}H NMR (400 MHz, DMSO) (Figure S8): ^{1}H NMR (400 MHz, DMSO) δ 8.95 (d, J = 7.7 Hz, 2H), 8.55 (d, J = 4.4 Hz, 2H), 8.29 (d, J = 6.8 Hz, 2H), 7.69 (dd, J = 7.2, 4.7 Hz, 2H), 7.37 (t, J = 7.4 Hz, 6H), 7.23 (dd, J = 15.0, 7.5 Hz, 14H), 7.08 (d, J = 7.1 Hz, 12H), 2.34 (s, 3H). Anal. Calcd for $C_{56}H_{43}CuN_4P_2$: C, 74.94; H, 4.83; N, 6.24%. Found: C, 75.38; H, 5.08; N, 6.46%.

Characterization methods

^{1}H NMR (400 MHz) were collected on a Bruker ACF-400 spectrometer and the NMR chemical shifts were recorded with deuterated CH_2Cl_2 or DMSO as solvent and tetramethylsilane as internal standard. Elemental analyses (C, H, O and N) were determined using a Bio-Rad elemental analysis system. The powder X-ray diffraction (PXRD) patterns were measured using a Bruker D8 Advance powder diffractometer at 40 kV and 40 mA with Cu Kα radiation (λ = 1.5418 Å), with a scan speed of 0.2 s per step and a step size of 0.02 (2θ). Absorption spectra were measured using a TU-1901 UV/vis spectrophotometer. PL spectra were obtained using an RF-5301PC spectrofluorimeter connected to a photomultiplier tube with a xenon lamp as the excitation source.

X-Ray crystallography

X-ray data for complexes **1b**, **2a** and **2b** were collected using a Bruker SMART APEX II CCD area detector diffractometer using graphite monochromated Mo K⍰ (λ= 0.71073 Å). The crystal structure was solved by direct methods and refined on F2 by full-matrix least-squares methods using the SHELXTL-97

program[19]. The hydrogen atom positions were calculated theoretically and included in the final cycles of refinement in a riding model along with attached carbon atoms. Complexes **1b** and **2a** belong to the triclinic space group P-1, and **2b** belongs to the Orthorhombic space group $Pna2_1$. The BF_4 anion in **1b** was found to display some degree of disorder and was refined successfully. A summary of the key crystallographic information is listed in Table 3. More detailed crystallographic data have been given in their cif files.

Table 3. Crystallographic data for complex **1b**, **2a** and **2b**

Complex	**1b**	**2a**	**2b**
Formula	$C_{57}H_{50}BCuF_4N_4O_2P_2$	$C_{56}H_{43}CuN_4O_2P_2$	$C_{56}H_{43}CuN_4P_2$
Formula weight	1035.30	929.42	897.42
Crystal form	Yellow, block	Orange, block	Red, block
Crystal system	Triclinic	Triclinic	Orthorhombic
Space group	P-1	P-1	$Pna2_1$
a/Å	10.3872(6)	13.0549(2)	19.491(4)
b/Å	14.4087(10)	13.6031(2)	25.892(5)
c/Å	18.4400(10)	14.2237(2)	8.9679(18)
α(°)	95.95(2)	73.0790(10)	90.00
β(°)	102.000(14)	75.2490(10)	90.00
γ(°)	109.680(13)	87.8950(10)	90.00
V / $Å^3$	2496.2(3)	2335.04(6)	4525.7(16)
Z / F(000)	2 / 1072	2 / 964	4 / 1864
Dc/mg.m^{-3}	1.377	1.322	1.317
μ/mm^{-1}	0.564	0.584	0.597
Crystal size/mm	0.20×0.40×0.58	0.21×0.21×0.19	0.20×0.27×0.40
θ range	3.02–25.01	1.61-25.10	3.15-25.00
Index range	$-12 \leqq h \leqq 10$ $-17 \leqq k \leqq 17$ $-20 \leqq l \leqq 21$	$-15 \leqq h \leqq 15$ $-16 \leqq k \leqq 15$ $-16 \leqq l \leqq 16$	$-23 \leqq h \leqq 13$ $-30 \leqq k \leqq 28$ $-10 \leqq l \leqq 10$
Reflections collected / unique [R(int)]	8481 / 6597	8270 / 7165	6495 / 4136
R, wR_2 ($I > 2\sigma(I)$)	0.0654, 0.1504	0.0459, 0.0974	0.0660, 0.0890
Goodness of fit, F^2	0.979	1.056	0.904
Largest diff. peak, hole/e $Å^3$	0.461, -0.343	0.802, -0.302	0.553, -0.351

Theoretical Calculations

The geometry optimization of the neutral copper(I) complexes **2a** and **2b** were performed using Gaussian 03 suite where the crystal structure data were used as the starting geometry. The calculations were carried out at the B3LYP/6-31G** level of the density functional theory (DFT). A 6-31G basis set was employed for C, H, O and N atoms, and a LANL2DZ basic set was implemented for Cu atom.

Acknowledgements

The authors are grateful for the financial support from the National Natural Science Foundation of China (No. 21302082 and 21271098), the Scientific Research Fund of Henan Provincial Education Department (No. 14B150057) and Program for Innovative Research Team (in Science and Technology) in University of Henan Province (14IRTSTHN008).

References

1 M. J. Leitl, F. R. Küchle, H. A. Mayer, L. Wesemann and H. Yersin, *J. Phys. Chem. A*, 2013, **117 (46)**, 11823; T. Hofbeck, U. Monkowius and H. Yersin, *J. Am. Chem. Soc.*, 2015, **137 (1)**, 399; Y. Sevryugina, O. Hietsoi and M. A. Petrukhina, *Chem. Commun.*, 2007, **37**, 3853; O. Hietsoi, C. Dubceac, A. S. Filatov and M. A. Petrukhina, *Chem. Commun.*, 2011, **47(24)**, 6939; O. Hietsoi, A. S. Filatov and M. A. Petrukhina, *Dalton Trans.*, 2011, **40(34)**, 8598; R. Starosta, M. Florek, J. Król, M. Puchalska and A. Kochel, *New J. Chem.*, 2010, **34(7)**, 1441.

2 C. Kutal, *Coord. Chem. Rev.*, 1990, **99**, 213; P. C. Ford, E. Cariati, J. Bourassa, *Chem. Rev.*, 1999, **99(12)**, 3625; D. V. Scaltrito, D. W. Thompson, J. A. O'Callaghan and G. J. Meyer,

Chem. Rev., 2000, **208(1)**, 243; H. Araki, K. Tsuge, Y. Sasaki, S. Ishizaka and N. Kitamura, *Inorg. Chem.*, 2005, **44(26)**, 9667; V. W. W. Yam and K. M. C. Wong, *Chem. Commun.*, 2011, **47(42)**, 11579; M. J. Leitl, F. R. Küchle, H. A. Mayer, L. Wesemann and H. Yersin, *J. Phys. Chem. A*, 2013, **117(46)**, 11823; T. Gneuß, M. J. Leitl, L. H. Finger, N. Rau, H. Yersin and J. Sundermeyer, *Dalton Trans.*, 2015, **44(18)**, 8506.

3 A. Bencini and V. Lippolis, *Coord. Chem. Rev.*, 2010, **254(17)**, 2096; X. Ma, X. Li, Y. E. Cha and L. P. Jin, *Cryst. Growth Des.*, 2012, **12 (11)**, 5227.

4 N. Armaroli, *Chem. Soc. Rev.*, 2001, **30(2)**, 113; M. Hashimoto, S. Igawa, M. Yashima, I. Kawata, M. Hoshino and M. Osawa, *J. Am. Chem. Soc.*, 2011, **133 (27)**, 10348.

5 D. G. Cuttell, S. M. Kuang, P. E. Fanwick, D. R. McMillin and R. A. Walton, J. Am. Chem. Soc., 2002, **124**, 6; R. B. Hou, T. H. Huang, X. J. Wang, X. F. Jiang, Q. L. Ni, L. C. Gui, Y. J. Fan and Y. L. Tan, Dalton Trans., 2011, **40**, 7551.

6 G. Accorsi, A. Listorti, K. Yoosaf and N. Armaroli, *Chem. Soc. Rev.*, 2009, **38(6)**, 1690.

7 C. E. A. Palmer and D. R. McMillin, *Inorg. Chem.*, 1987, **26**, 3837; M. T. Miller, P. K. Gantzel and T. B. A. Karpishin, *J. Am. Chem. Soc.*, 1999, **121**, 4292; D. G. Cuttell, S. M. Kuang and P. E. Fanwick, *J. Am. Chem. Soc.*, 2001, **124(1)**, 6; A. Kaeser, M. Mohankumar, J. Mohanraj, F. Monti, M. Holler, J. Cid, O. Moudam, I. Nierengarten, L. Karmazin-Brelot, C. Duhayon, B. Delavaux-Nicot, N. Armaroli and J. Nierengarten, *Inorg. Chem.*, 2013, **52**, 12140; R. Starosta, M. Puchalska, J. Cybińska, M. Barys and A. V. Mudring, *Dalton Trans*, 2011, **40(11)**, 2459.

8 Y. Xiong, X. F. He, X. H. Zou, J. Z. Wu, X. M. Chen, L. N. Ji, R. H. Li, J. Y. Zhou and K. B. Yu, *J. Chem. Soc., Dalton Trans.*, 1999, 19; Q. Zhao, S. J. Liu, M. Shi, F. Y. Li, H. Jing, T. Yi and C. H. Huang, *Organometallics*, 2007, **26**, 5922; A. Quaranta, F. Lachaud, C. Herrero, R. Guillot, M. F. Charlot, W. Leibl and A. Aukauloo. *Chem. Eur. J.*, 2007, **13**, 8201; X. L. Wang, Y. Q. Chen, Q. Gao, H. Y. Lin, G. C. Liu, J. X. Zhang and A. X. Tian, *Cryst. Growth Des.*, 2010, **10 (5)**, 2174; Y. Wei, K. Wu, J. He, W. Zheng and X. Xiao, *CrystEngComm*, 2011, **13**, 52; L. Wang, L. and Ni J. Yao, *Polyhedron*, 2013, **59**, 115.

9 H. Chao, Y. X. Yuan and L. N. Ji, *Trans. Met. Chem.*, 2004, **29**, 774; Y. J. Huang and L. Ni, *Chin. J. Inorg. Chem.*, 2011, **27(8)**, 1649; R. O. Bonello, I. R. Morgan, B. R. Yeo, L. E. L. Jones, B. M. Kariuki, I. A. Fallis and S. J. A. Pope, *J. Organomet. Chem.*, 2014, **749**, 150.

10 C. Janiak. *Dalton Trans.*, 2000, 3885; J. Min, Q. Zhang, W. Sun, Y. Cheng and L. Wang, *Dalton Trans.*, 2011, **40**, 686; C. W. Hsu, C. C. Lin, M. W. Chung, Y. Chi, G. H. Lee, P. T. Chou, C. H. Chang and P. Y. Chen, *J. Am. Chem. Soc.* 2011, **133**, 12085.

11 A. Bhattacharyya, P. K. Bhaumik, A. Bauzá, P. P. Jana, A. Frontera, M. G. B. Drew, S. Chattopadhyay, *RSC Adv.*, 2014, **4**, 58643; H. L. S. Wong, D. R. Allan, N. R. Champness, J. McMaster, M. Schröder and A. J. Blake, *Angew. Chem. Int. Ed.*, 2013, **52(19)**, 5093; R. Banik, S. Roy, A. Bauza, A. Frontera, S. Das, *RSC Adv.*, 2015, **5**, 10826.

12 S. M. Kuang, D. G. Cuttell, D. R. McMillin, P. E. Fanwick and R. A. Walton, *Inorg. Chem.*, 2002, **41(12)**, 3313.

13 H. Nitadori, L. Ordronneau, J. Boixel, D. Jacquemin, A. Boucekkine, A. Singh, M. Akita, I. Ledoux, V. Guerchais and H. L. Bozec, *Chem. Commun.*, 2012, **48**, 10395; X. L. Li, Y. B. Ai, B. Yang, J. Chen, M. Tan, X. L. Xin and Y. H. Shi, *Polyhedron*, 2012, **35(1)**, 47; R. Marion, F. Sguerra, F. D. Meo, E. Sauvageot, J. F. Lohier, R. Daniellou, J. L. Renaud, M. Linares, M. Hamel and S. Gaillard, *Inorg. Chem.*, 2014, **53 (17**), 9181.

14 T. McCormick, W. L. Jia, S. Wang, *Inorg. Chem.* 2006, **45**, 147; S. Sakaki, H. Mizutani, Y. I. Kase, K. J. Inokuchi, T. Arai, T. J. Hamada, *Chem. Soc., Dalton Trans.*, 1996, 1909.

15 E. D. Hedegård, J. Bendix and S. P. Sauer, *J. Mol. Struct. THEOCHEM*, 2009, **913(1)**, 1.

16 G. F. Manbeck, W. W. Brennessel and R. Eisenberg, *Inorg. Chem.*, 2011, **50**, 3431; M. G. Crestani, G. F. Manbeck, W. W. Brennessel, T. M. McCormick and R. Eisenberg, *Inorg. Chem.*, 2011, **50**, 7172; S. Perruchas, C. Tard, X. F. Le Goff, A. Fargues, A. Garcia, S. Kahlal, J. Y. Saillard, T. Gacoin and J. P. Boilot, *Inorg. Chem.*, 2011, **50**, 10682.

17 E. A. Steck and A. R. Day, *J. Am. Chem. Soc.*, 1943, **65 (3**), 452; H. Xu, K. C. Zheng, H. Deng, L. J. Lin, Q. L. Zhang and L. N. Ji, *New J. Chem.*, 2003, **27(8)**, 1255; J. Liu, W. J. Mei, L. J. Lin, Q. L. Zhang, H. Chao, F. C. Yun, L. N. Ji, *Inorg. Chim. Acta*, 2004, **357(1)**, 285.

18 G. J. Kubas, B. Monzyk, A. L. Crumbliss, *Inorg. Synth.* 1979, **19**, 90.

19 G. M. Sheldrick, SHELXTL, version 5.1, Bruker Analytical X-ray Systems, Inc., Madision, WI 1997.

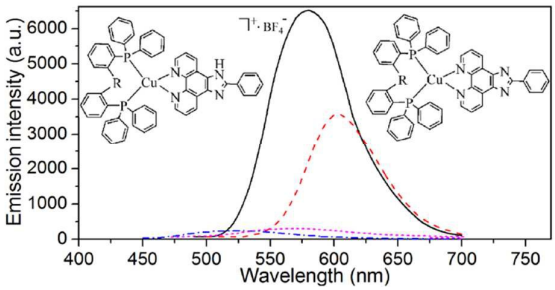

Deprotonation of imidazole-phenanthroline ligand leads to an entirely different luminescence properties of neutral Cu(I) complexes compared with ionic Cu(I) complexes.